SCIENCE CHINA
Information Sciences

• RESEARCH PAPER •

October 2020, Vol. 63 202302:1–202302:10
https://doi.org/10.1007/s11432-020-2972-0

Integrated multi-scheme digital modulations of spoof surface plasmon polaritons

Lepeng ZHANG[1], Haochi ZHANG[1], Min TANG[2*], Peihang HE[1], Lingyun NIU[1], Liangliang LIU[3], Jiayuan LU[1], Wenxuan TANG[1], Junfa MAO[2] & Tiejun CUI[1*]

[1]*State Key Laboratory of Millimeter Waves, Southeast University, Nanjing 210096, China;*
[2]*Key Laboratory of Ministry of Education of China for Research of Design and Electromagnetic Compatibility of High Speed Electronic Systems, Shanghai Jiao Tong University, Shanghai 200240, China;*
[3]*Research Center of Applied Electromagnetics, School of Electronic and Information Engineering, Nanjing University of Information Science and Technology, Nanjing 210044, China*

Received 31 March 2020/Accepted 24 June 2020/Published online 16 September 2020

Abstract The future wireless communications require different kinds of modulation functions to be integrated in a single intelligent device under different scenarios. Here, we propose a multi-scheme digital modulator to achieve this goal based on integrated spoof surface plasmon polaritons (SPP) in different frequency bands. By constructing switchable spoof SPP units, the propagating wave in the proposed spoof SPP waveguide can be manipulated in amplitude domain, frequency domain, and phase domain. As a proof of concept, the integrated multi-scheme digital modulator is experimentally verified to achieve at least three kinds of modulations, including amplitude shift keying, phase shift keying, and frequency shift keying, in a single digital spoof plasmonic waveguide. The simulated and measured results show that the modulator has excellent property of field confinement and is capable of frequency-domain modulation. Hence, the multi-scheme modulation property makes the proposed SPP digital modulator be an effective and reliable candidate for efficient manipulations of SPP waves and for advanced modulation technology.

Keywords spoof surface plasmon polaritons, dynamic manipulation, multi-scheme modulation, dispersion engineering, frequency modulation

Citation Zhang L P, Zhang H C, Tang M, et al. Integrated multi-scheme digital modulations of spoof surface plasmon polaritons. Sci China Inf Sci, 2020, 63(10): 202302, https://doi.org/10.1007/s11432-020-2972-0

1 Introduction

Modulation technologies based on electromagnetic (EM) characteristics such as amplitude, phase, and frequency are the basis of modern communications. Among them, the amplitude shift keying (ASK), phase shift keying (PSK), and frequency shift keying (FSK) are regarded as the most fundamental schemes, showing their irreplaceable advantages in different aspects such as power consumption, spectrum occupancy, and efficiency [1–3]. For example, ASK has the advantages of low cost and low power consumption; FSK is used in data transmission due to its low attenuation; while PSK has the strongest anti-interference capability and has been widely used in space communications. Hence, to meet the requirement of different potential applications, the future intelligent communication device should have the ability to carry out multi-scheme modulations in a compact space. For example, from the perspective of communication security, when one kind of modulated signal is interfered, the multi-scheme modulators can generate another kind of modulation signal to keep the communication going.

* Corresponding author (email: tm222@sjtu.edu.cn, tjcui@seu.edu.cn)

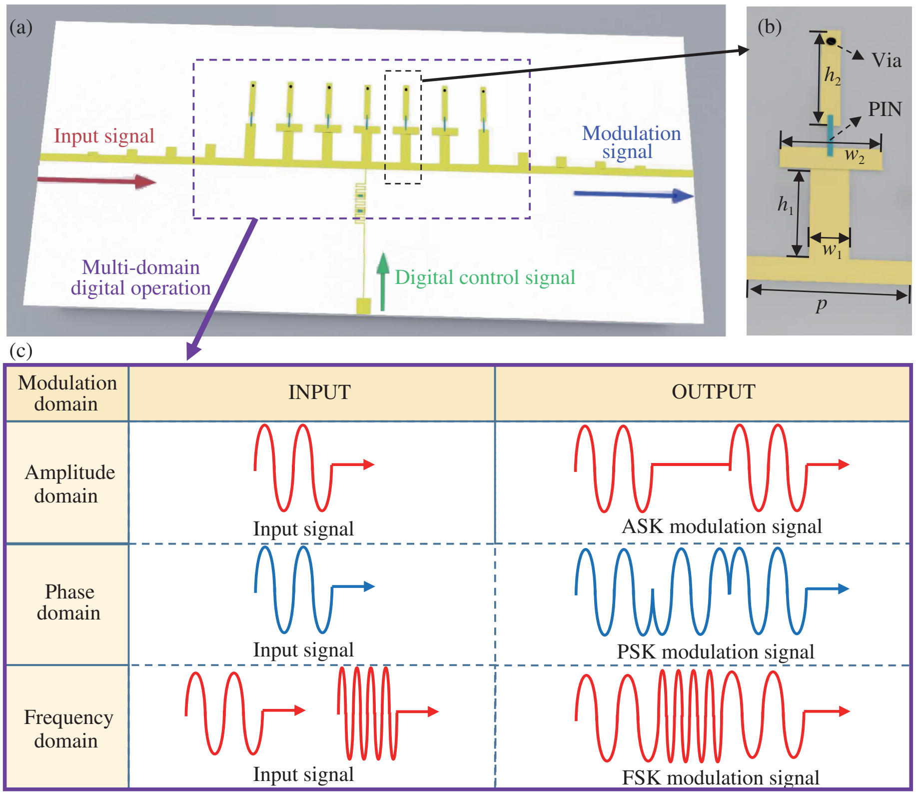

Figure 1 (Color online) The proposed SPP structure and resulting multi-scheme modulations. (a) The multi-scheme-modulation SPP waveguide, whose main part is outlined in the purple dashed line. (b) The schematic diagram of a single switchable SPP unit, in which the period $p = 6$ mm, radius of metal hole $r = 0.2$ mm, width of metallic bar $w_1 = 1.5$ mm, $w_2 = 3.5$ mm, height of metallic bar $h_1 = 4$ mm, and height of upper metallic bar $h_2 = 5$ mm. (c) The schematic diagram of multi-scheme modulations. In different modulation schemes, different modulation SPP signals are generated.

Over the past decades, the emergence of metamaterials or metasurfaces provides the possibility of manipulating the EM waves flexibly [4–10]. Owing to the unique and excellent physical properties such as negative index of refraction [11], near-zero index of refraction [12–14], and extremely strong chirality [15], the metamaterials have attracted more dramatic attention. Introducing the concept of manipulating surface waves at low frequencies, spoof surface plasmon polaritons (SPP) have been proposed to manipulate the EM waves in subwavelength scale [16–21]. Owing to their distinctive properties of strong field confinement and enhancement, the spoof SPP metamaterials promise useful applications in miniaturized devices [22, 23], low-cross-talk waveguides [24–26], and others [27–33]. However, limited by their fixed structure and inherent analog nature, the traditional metamaterials (including spoof SPP metamaterials) are difficult to achieve dynamic manipulations, and even more difficult to establish connection with digital modulations.

In order to solve the above problems, digital technology has recently been introduced to metamaterials [34–42]. This concept was also extended to the subwavelength scale to control the spoof SPPs [39], which pioneers the concept of digital spoof SPPs and provides the possibility of manipulating the spoof SPPs dynamically. However, the scheme in Ref. [39] cannot be used to realize frequency-domain modulations, which plays a fundamental and important role in the modern information systems.

In this paper, a spoof SPP digital modulator is realized by introducing positive-intrinsic-negative (PIN) junction diode into the plasmonic metamaterials to integrate the above three kinds of most fundamental modulation functions (ASK, PSK, and FSK) in a single device, as shown in Figure 1(a). First, a switchable SPP unit is constructed and the dispersion engineering is demonstrated analytically in Section 2. Then, we propose a multi-scheme-modulation SPP waveguide by arranging the SPP units and measure the transmission spectra and field distributions in Section 3. In Section 4, the measurement of the time-domain waveform of the multi-scheme-modulation waveguide is implemented. Finally, we

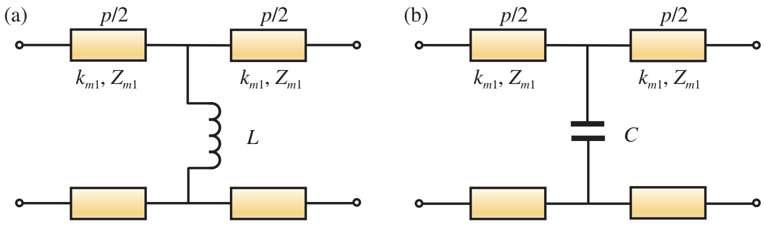

Figure 2 (Color online) Equivalent circuit models of the proposed SPP unit with (a) short-circuit stub and (b) open-circuit stub.

discuss conclusion in Section 5.

2 Switchable SPP unit and dispersion engineering

To manipulate spoof SPPs in multiple schemes based on single structure, a specially designed SPP unit is required, as shown in Figure 1, which can provide different physical responses according to different external excitation signals. The signals propagating in the proposed SPP waveguide can also be manipulated flexibly in different schemes (ASK, PSK, and FSK) by external digital signals, as shown in Figure 1(c).

In order to realize switchable states of the SPP unit, a PIN diode is introduced, which can be easily controlled by external voltages to achieve two distinctly physical responses, "ON" state and "OFF" state. It is worth mentioning that the PIN diode has been studied for configurability of microwave components in industry manuals [43]. However, the previous work has not focused on the modulation of SPPs. Inspired by the conventional corrugated spoof SPP unit, a novel unit supporting controllable spoof SPPs is constructed by the PIN diode and subwavelength-scale planner metallic structures, as shown in Figure 1(b). It is worth mentioning that the outermost metal structure is connected to the metal ground by a metallic via, which is different from the scheme in Ref. [39].

To explain the working principle, the proposed SPP unit is investigated using circuit topology, which can be modeled as a slow-wave transmission line (TL) loaded with short-circuit stubs ("ON" state) or open-circuit stubs ("OFF" state), as shown in Figure 2. The main TL is modeled using a microstrip with propagation constant k_{m1} and impedance Z_{m1}, and the shunt branches are regarded as admittance Y. For Bloch waves propagating in a periodic structure, the dispersion-curve formula is expressed as [40]

$$\cos(kp) = \cos(k_{m1}p) + \mathrm{j}\frac{Z_{m1}Y}{2}\sin(k_{m1}p). \tag{1}$$

For the "ON" state, as shown in Figure 2(a), the proposed unit is actually loaded with the short-circuit stub, which is characterized as an effective inductance L:

$$L = \frac{Z_{\text{short}}}{\mathrm{j}w} = \frac{Z_{m2}\tan(k_{m2}h)}{w}. \tag{2}$$

In this case, the shunt admittance Y is

$$Y_{\text{short}} = \frac{1}{\mathrm{j}wL} = \frac{1}{\mathrm{j}Z_{m2}\tan(k_{m2}h)}. \tag{3}$$

For the "OFF" state, as shown in Figure 2(b), the proposed unit is actually loaded with the open-circuit stub, which is characterized as an effective capacitor C:

$$C = \frac{1}{\mathrm{j}wZ_{\text{open}}} = \frac{1}{wZ_{m2}\cot(k_{m2}h_2)}. \tag{4}$$

In this case, the shunt admittance Y is

$$Y_{\text{open}} = \mathrm{j}wC = \frac{\mathrm{j}}{Z_{m2}\cot(k_{m2}h_2)}. \tag{5}$$

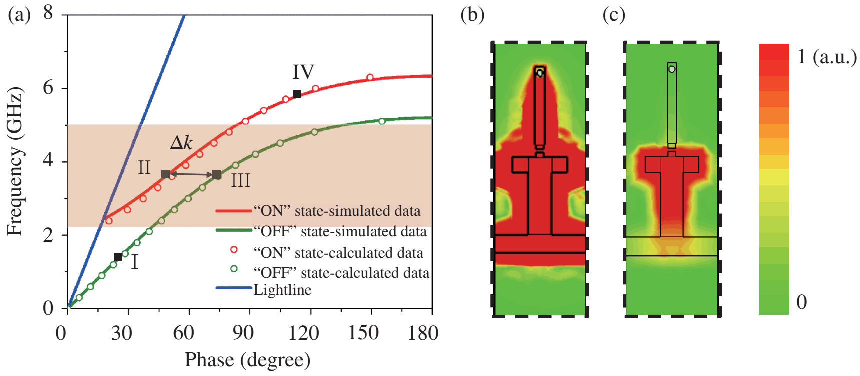

Figure 3 (Color online) (a) Dispersion curves of the proposed SPP unit in the "ON" and "OFF" states; (b), (c) the Eigen-mode field distributions of the SPP units in the "ON" and "OFF" states at 3.7 GHz.

Substituting Eqs. (3) and (5) into (1), the calculated dispersion curves can be obtained, as shown in Figure 3(a).

It is worth noting that the above circuit model can be used to illustrate the principle but the quantitative relationship between circuit parameters and structure parameters has not been established. In order to determine the structure parameters, the proposed SPP unit is investigated through eigenmode simulations. Based on the finite-element analysis of the eigenmode, the dispersion curves of the proposed unit with "ON" and "OFF" states are displayed in Figure 3(a), where the metal and dielectric substrate are selected as copper and Rogers RO4350B, respectively. To simulate the switchable characteristics, the "ON" state of the PIN diode is considered as a metallic material and the "OFF" state is treated as a dielectric with high relative permittivity. As shown in Figure 3(a), the red and green lines respectively characterize the dispersion curves of the "ON" and "OFF" states, which matches the calculated dispersion curves well, confirming the circuit theoretical analysis. It is noted that these two dispersion curves gradually separate from the light line in vacuum and asymptotically approach two different cut-off frequencies, behaving like the natural SPP modes at the optical frequencies. Thus, a lower cut-off frequency of the dispersion curve in the "ON" state can be realized creatively by introducing the metallized via holes, which is the key to manipulate the spoof SPPs in the frequency domain.

Due to the excellent property of the proposed structure to engineer the characteristics of spoof SPPs flexibly by changing the parameters, the operating frequency has the advantage of customizability. By changing the structure parameters, such as $h1$ and $h2$, the operating frequency can be adjustable. By designing the parameters carefully, two switchable dispersion curves make it possible to manipulate the SPP waves in three different schemes. In the case of point I or IV as shown in Figure 3(a), only one state supports the transmission of spoof SPP signals but the other does not, which achieves the ASK scheme easily. In the case of points II and III, both states support the SPP signal transmissions but correspond to different phase responses. The designed phase difference is exactly 180°, which can realize the PSK scheme. When two signals of specific frequencies (such as the two frequencies in points I and IV) are input to the proposed unit structure, each state supports the transmission of the signal at one frequency and blocks the transmission at the other frequency, which contributes to the FSK scheme. Hence, the dynamic manipulations of the signal frequencies can be implemented. Based on the proposed SPP unit, it is possible to realize multi-scheme modulations, including ASK, PSK, and FSK.

From the physical view, the switchable states of the PIN diode actually control the flow of current between the upper and lower metallic slices. In other words, the reconfigurable physical structure leads to the adjustable physical responses. When the PIN diode is at the "ON" state, the EM energy distributes through diodes to the upper metallic slices, as shown in Figure 3(b). The lower-frequency EM wave finally flows to the metal ground through the metal via, and that is the reason why the low cut-off frequency appears in the dispersion curve of the "ON" state. Owing to the inductive effect of the metal groove structure, the higher-frequency EM energy is blocked into the metal ground and the transmission of SPP wave is still supported. In contrast, when the PIN diode is at the "OFF" state, the EM energy

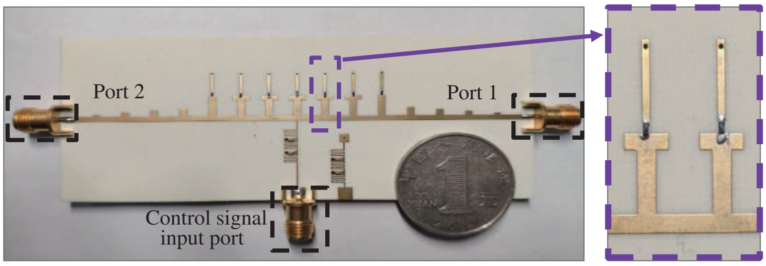

Figure 4 (Color online) Photographs of the fabricated prototype.

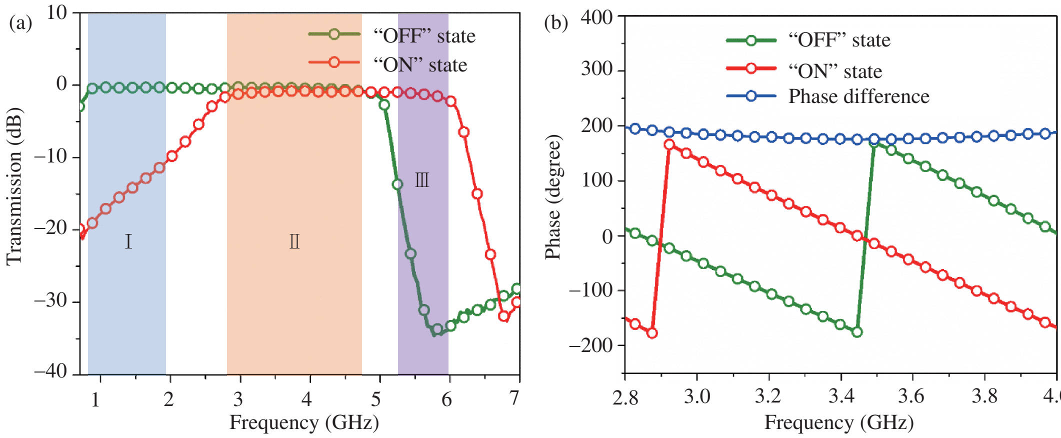

Figure 5 (Color online) The measured transmission amplitude (a) and phase spectra (b) of the proposed SPP waveguide in the "ON" and "OFF" states.

is prevented from the upper metallic slices, as shown in Figure 3(c), hence the dispersion curve presents a typical low-pass type. Clearly, the EM energy in both two states is distributed in the vicinity of the metal structure, which behaves the strong field confinement characteristics of the spoof SPPs.

3 Structure realization of multi-scheme modulations

The proposed switchable SPP unit provides the possibility of manipulating the SPP signals in multiple schemes based on a single structure. However, the discrete physical responses not only need to be constructed, but also controlled by the external signals. Inspired by this idea, a multi-scheme-modulation SPP waveguide is proposed by arranging the SPP units with period p along the x axis on the top surface of dielectric substrate made by Rogers RO4350B and metallic ground on the bottom surface, as shown in Figure 4. The PIN diode is selected as MADP-000907-14020x. Applying different DC bias voltages between two terminals of the PIN diode, the "ON" and "OFF" states can be switched. In order to avoid the high-frequency leakage to the bias port and metallic ground, a choke structure is designed, which is composed of meander lines and lumped chip capacitors. Besides, two momentum compensations are designed to reduce the mismatch between the quasi-transverse EM mode and SPP mode using a planar gradient index structure.

To verify the performance of the proposed SPP waveguide, the transmission spectra and near-field distributions are measured by a vector network analyzer and near-field scanning mapper, respectively, as shown in Figures 5 and 6. In the measured S-parameter results in Figure 5(a), three frequency bands are applied to achieve three different modulation functions. In region I or III, there is only one state, in which the EM signal can be transmitted and the amplitude of the signals can be conveniently controlled by the external voltage to switch the "ON" and "OFF" states. It is worth mentioning that the proposed multi-scheme-modulation SPP waveguide allows the amplitude at lower frequencies rather than only at relative higher frequencies. More importantly, when two signals of different frequencies (one is located in region I

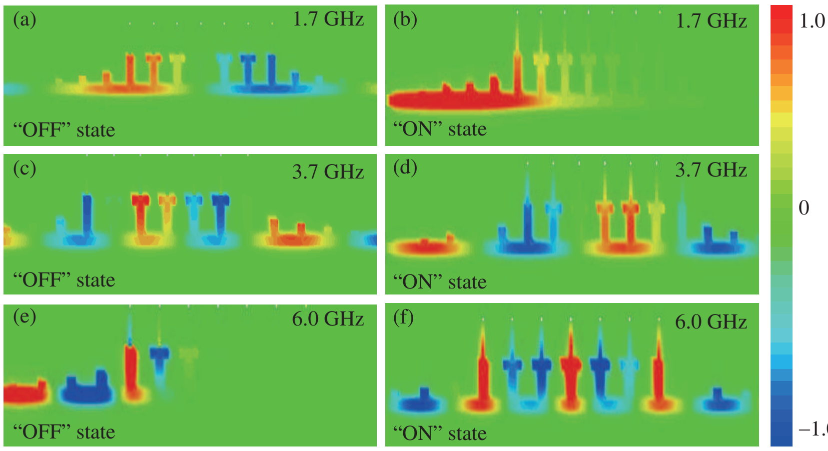

Figure 6 (Color online) The simulated near-field distributions of the proposed SPP waveguide in the "OFF" state ((a), (c) and (e)) and "ON" state ((b), (d) and (f)).

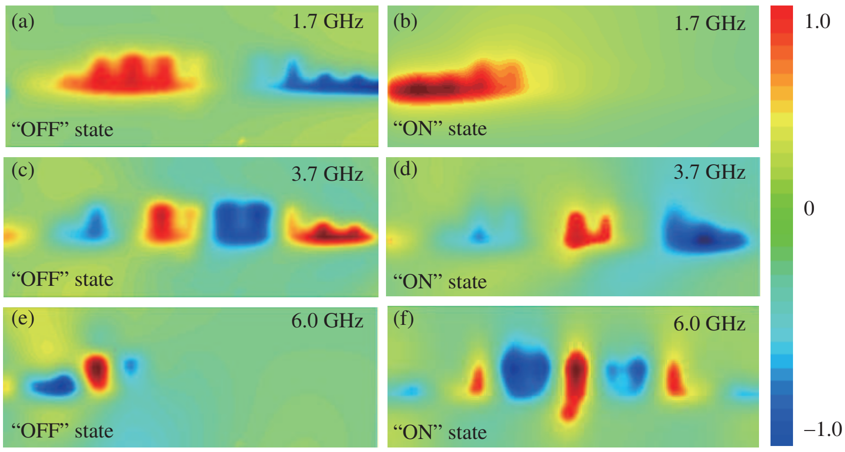

Figure 7 (Color online) The measured near-field distributions of the proposed SPP waveguide in the "OFF" state ((a), (c) and (e)) and "ON" state ((b), (d) and (f)).

and the other is in region III) are fed into the proposed SPP waveguide at the same time, only one kind of frequency signal can transmit in each state. Hence, the frequency of the signal can be dynamically modulated by the external bias voltage, which has never been reported in previous research. In region II, both states support the EM signal transmissions but their phase responses are different. The inherent wavenumber difference between the two states can be accumulated along the propagation direction and the phase difference may achieve 180° by carefully designing the length of the SPP waveguide, as shown in Figure 5(b), which makes the phase modulation possible.

The near-field distributions also demonstrate the ability of the proposed SPP waveguide to manipulate the EM signal in multiple schemes. Figures 6 and 7 show the simulated and measured results, respectively. As displayed in Figures 6 and 7, at 1.7 GHz, most EM energy can go through the proposed SPP waveguide in the "OFF" state while little EM energy is received by the output port in the "ON" state. However, at 6 GHz, the EM behavior is actually opposite. That is to say, the switchable states controlled by the external bias voltage have remarkable manipulation ability of EM signals. At 3.7 GHz, the EM signals can be transmitted well in both "ON" and "OFF" states. More importantly, the outputs of such two states have opposite responses. Hence the EM behaviors obtained from the near-field distributions are consistent with the S-parameter results and dispersion characteristics, further confirming the aforementioned theoretical analysis from a more visual perspective. It is noted that the proposed multi-scheme SPP waveguide also keeps the excellent ability of field confinement, in which the EM energy in all states is confined around the metal structure obviously.

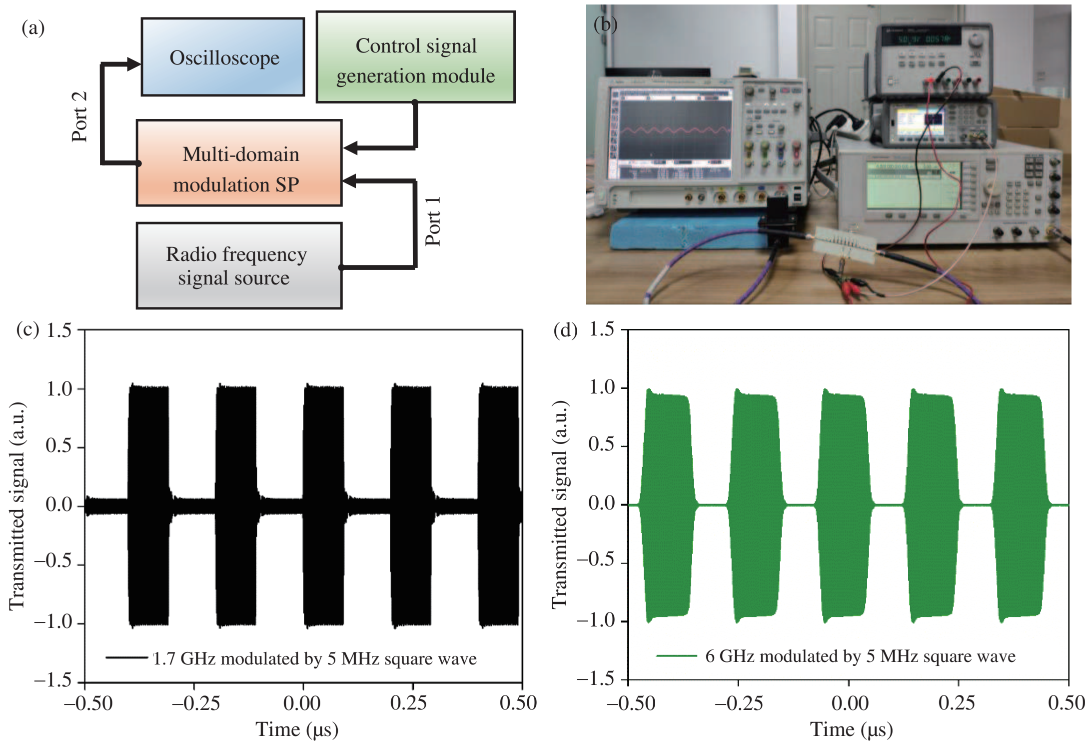

Figure 8 (Color online) (a) The schematic diagram of measurement system for time-domain spectra; (b) the photograph of the measurement setup; (c), (d) the measured time-domain spectra of transmitted signals in the amplitude-modulation scheme modulated by 5 MHz square wave.

4 Experimental verification of the multi-scheme modulation

By means of the measured transmission spectra and near-field distributions, the ability of manipulating the EM signal in multiple schemes of the proposed SPP waveguide is analyzed in details. However, the ultimate purpose of manipulating EM signals is to generate the modulated signals. Hence, we show experimental demonstration and performance verification of spoof SPP signals modulated directly by a square wave. For this reason, the measurement of the time-domain waveform of the multi-scheme-modulation waveguide is implemented. The experimental system is described in Figure 8(a) and the photograph of the measurement setup is shown in Figure 8(b). To verify the modulation ability of the proposed SPP waveguide more intuitively, the experiments of time-domain spectroscopies in multi-scheme (ASK, PSK, and FSK) are demonstrated in turns.

In the ASK scheme, we observe that the transmitted signals at 1.7 GHz are modulated by the 5 MHz square waves, as shown in Figure 8(c), which display a significant transmission ratio (more than 10 times) between the “ON” and “OFF” states in the time domain. As shown in Figure 8(d), the EM signal at 6 GHz can also be modulated by the 5 MHz square wave. The amplitude variation of the EM signal carries the transmitted information and the amplitude modulation is fully controlled by the external voltage bias. Remarkably, the amplitude modulation in both higher and lower frequency bands has been proved, expanding the available frequency range.

Based on the same fabricated sample, the experiment of phase modulation is also carried out. As shown in Figure 9, the signal waveform at 3.7 GHz modulated by the 5 MHz square wave is displayed. It is noted that the phases of the time-domain signals are reversed when switching the “ON” and “OFF” states for most parts of the time. Hence, the information to be transmitted is reflected in the phase behavior of the high-frequency signal. The solid line in the figure shows the theoretical curve in both states, which fits the measured data perfectly.

Furthermore, the experiment of frequency modulation is implemented by using the same sample. The signal modulated by the 5 MHz square wave is displayed in Figure 10. Clearly, one signal at 1.7 GHz

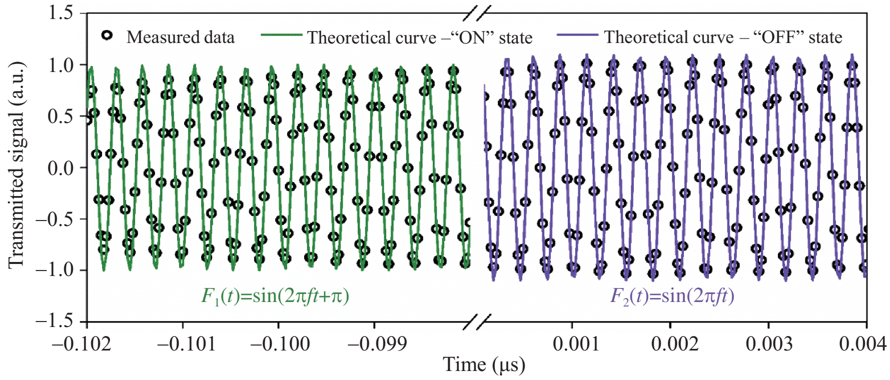

Figure 9 (Color online) The measured time-domain spectra of transmitted signals in the phase-modulation scheme under different inputs. The incident signal at 3.7 GHz modulated by 5 MHz square wave.

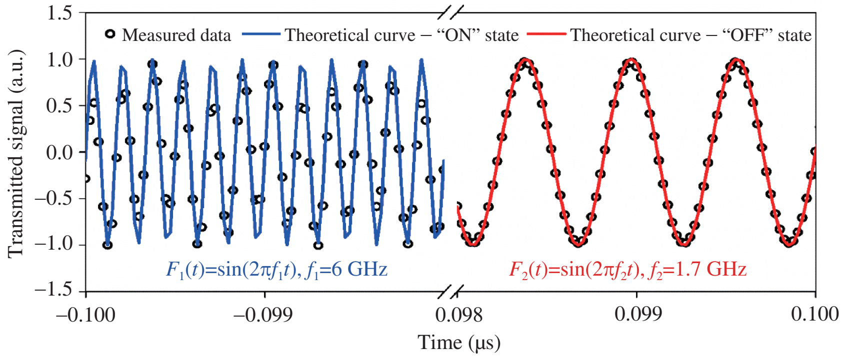

Figure 10 (Color online) The measured time-domain spectra of transmitted signals in the frequency-modulation scheme. The incident signals at 1.7 GHz and 6 GHz modulated by 5 MHz square wave.

or 6 GHz can be transmitted through this plasmonic waveguide at the same time. The frequency of the EM signals changes with the external voltage switching, and in this case the frequency variation of signal carries the information. In conclusion, all amplitude modulation, phase modulation and frequency modulation have been realized using a single sample with different operating frequencies, and the experimental results of multi-scheme modulations agree well with the theoretical curves.

5 Conclusion

An integrated multi-scheme digital modulator based on spoof SPPs has been investigated. By introducing PIN diodes into spoof SPP waveguide, the switchable SPP unit was constructed and the dispersion engineering was demonstrated analytically. The signal propagating in the proposed SPP waveguide can be manipulated flexibly in different schemes (ASK, PSK, and FSK) and the time-domain waveforms were displayed in details. The proposed multi-scheme modulation SPP waveguide not only makes up the lack of frequency-domain modulation but also broadens the frequency range of amplitude modulation. More importantly, the integrated multi-scheme modulations of SPP signals has been implemented on a single sample, which provides a novel solution to realize more flexible and secure communication systems.

Acknowledgements This work was supported by National Key Research and Development Program of China (Grant Nos. 2017YFA0700201, 2017YFA0700202, 2017YFA0700203), National Natural Science Foundation of China (Grant Nos. 61571117, 61631007, 61701108, 61871127), and the 111 Project (Grant No. 111-2-05).

References

1 Raymo F M. Digital processing and communication with molecular switches. Adv Mater, 2002, 14: 401–414

2 Driessen P F, Greenstein L J. Modulation techniques for high-speed wireless indoor systems using narrowbeam antennas. IEEE Trans Commun, 1995, 43: 2605–2612
3 Gong X X, Peng Y H, Liu Y J, et al. Novel multi-band DFT-spread OFDM-PON systems based on intensity modulation and direct detection for cloud computing. Photon Netw Commun, 2016, 31: 550–558
4 Zheludev N I, Kivshar Y S. From metamaterials to metadevices. Nat Mater, 2012, 11: 917–924
5 Pendry J B, Aubry A, Smith D R, et al. Transformation optics and subwavelength control of light. Science, 2012, 337: 549–552
6 Yu N F, Genevet P, Kats M A, et al. Light propagation with phase discontinuities: generalized laws of reflection and refraction. Science, 2011, 334: 333–337
7 Yu N F, Capasso F. Flat optics with designer metasurfaces. Nat Mater, 2014, 13: 139–150
8 AbdollahRamezani S, Arik K, Khavasi A, et al. Analog computing using graphene-based metalines. Opt Lett, 2015, 40: 5239
9 Li W, Valentine J. Metamaterial perfect absorber based hot electron photodetection. Nano Lett, 2014, 14: 3510–3514
10 Wakatsuchi H, Long J, Sievenpiper D F. Waveform selective surfaces. Adv Funct Mater, 2019, 29: 1806386
11 Shelby R A. Experimental verification of a negative index of refraction. Science, 2001, 292: 77–79
12 Alú A, Silveirinha M G, Salandrino A, et al. Epsilon-near-zero metamaterials and electromagnetic sources: tailoring the radiation phase pattern. Phys Rev B, 2007, 75: 155410
13 Yang X D, Hu C Y, Deng H X, et al. Experimental demonstration of near-infrared epsilon-near-zero multilayer metamaterial slabs. Opt Express, 2013, 21: 23631
14 Hwang R B, Hsu N C, Chin C Y. A spatial beam splitter consisting of a near-zero refractive index medium. IEEE Trans Antenna Propag, 2012, 60: 417–420
15 Plum E, Zhou J F, Dong J F, et al. Metamaterial with negative index due to chirality. Phys Rev B, 2009, 79: 035407
16 Pendry J B, Martin-Moreno L, Garcia-Vidal F J. Mimicking surface plasmons with structured surfaces. Science, 2004, 305: 847–848
17 Hibbins A P, Evans B R, Sambles J R. Experimental verification of designer surface plasmons. Science, 2005, 308: 670–672
18 Garcia-Vidal F J, Martín-Moreno L, Pendry J B. Surfaces with holes in them: new plasmonic metamaterials. J Opt A-Pure Appl Opt, 2005, 7: 97–101
19 Maier S A, Andrews S R, Martín-Moreno L, et al. Terahertz surface plasmon-polariton propagation and focusing on periodically corrugated metal wires. Phys Rev Lett, 2006, 97: 176805
20 Shen X P, Cui T J, Martin-Cano D, et al. Conformal surface plasmons propagating on ultrathin and flexible films. Proc Natl Acad Sci USA, 2013, 110: 40–45
21 Shen X P, Cui T J. Planar plasmonic metamaterial on a thin film with nearly zero thickness. Appl Phys Lett, 2013, 102: 211909
22 Kabashin A V, Evans P, Pastkovsky S, et al. Plasmonic nanorod metamaterials for biosensing. Nat Mater, 2009, 8: 867–871
23 Kianinejad A, Chen Z N, Qiu C W. Low-loss spoof surface plasmon slow-wave transmission lines with compact transition and high isolation. IEEE Trans Microw Theory Techn, 2016, 64: 3078–3086
24 Zhang H C, Liu S, Shen X P, et al. Broadband amplification of spoof surface plasmon polaritons at microwave frequencies. Laser Photonics Rev, 2015, 9: 83–90
25 Tang W X, Zhang H C, Ma H F, et al. Concept, theory, design, and applications of spoof surface plasmon polaritons at microwave frequencies. Adv Opt Mater, 2019, 7: 1800421
26 Bian Y S, Gong Q H. Highly confined guiding of low-loss plasmon waves in hybrid metal-dielectric slot waveguides. Nanotechnology, 2014, 25: 345201
27 Yu N F, Wang Q J, Kats M A, et al. Designer spoof surface plasmon structures collimate terahertz laser beams. Nat Mater, 2010, 9: 730–735
28 Gao Z, Wu L, Gao F, et al. Spoof plasmonics: from metamaterial concept to topological description. Adv Mater, 2018, 30: 1706683
29 Zhang H C, Zhang L P, He P H, et al. A plasmonic route for integrated wireless communication of sub-diffraction-limited signals. Light Sci Appl, 2020, 9: 113
30 Ma H F, Shen X P, Cheng Q, et al. Broadband and high-efficiency conversion from guided waves to spoof surface plasmon polaritons. Laser Photonics Rev, 2014, 8: 146–151
31 Gao X X, Zhang H C, He P H, et al. Crosstalk suppression based on mode mismatch between spoof SPP transmission line and microstrip. IEEE Trans Compon Packag Manufact Technol, 2019, 9: 2267–2275
32 Gao X X, Zhang J J, Zhang H C, et al. Dynamic controls of second-harmonic generations in both forward and backward modes using reconfigurable plasmonic metawaveguide. Adv Opt Mater, 2020, 8: 1902058
33 Hang He P, Zhang H C, Gao X X, et al. A novel spoof surface plasmon polariton structure to reach ultra-strong field confinements. Opto-Electron Adv, 2019, 2: 190001
34 Cui T J, Qi M Q, Wan X, et al. Coding metamaterials, digital metamaterials and programmable metamaterials. Light Sci Appl, 2014, 3: 218
35 Cui T J. Microwave metamaterials. Nat Sci Rev, 2018, 5: 134–136
36 Majumder A, Shen B, Polson R, et al. Ultra-compact polarization rotation in integrated silicon photonics using digital metamaterials. Opt Express, 2017, 25: 19721
37 Zhang L, Chen X Q, Liu S, et al. Space-time-coding digital metasurfaces. Nat Commun, 2018, 9: 4334

38 Zhao J, Yang X, Dai J Y, et al. Programmable time-domain digital-coding metasurface for non-linear harmonic manipulation and new wireless communication systems. Natl Sci Rev, 2019, 6: 231–238
39 Zhang H C, Cui T J, Luo Y, et al. Active digital spoof plasmonics. Natl Sci Rev, 2020, 7: 261–269
40 Zhang H C, Cui T J, Xu J, et al. Real-time controls of designer surface plasmon polaritons using programmable plasmonic metamaterial. Adv Mater Technol, 2017, 2: 1600202
41 Wang M, Ma H F, Wu L W, et al. Hybrid digital coding metasurface for independent control of propagating surface and spatial waves. Adv Opt Mater, 2019, 11: 1900478
42 Ma M L, Li Z, Liu W W, et al. Optical information multiplexing with nonlinear coding metasurfaces. Laser Photonics Rev, 2019, 13: 1900045
43 Callsen H, Meinel H H, Hoefer W J R. p-i-n diode control devices in E-plane technique. IEEE Trans Microw Theory Techn, 1989, 37: 307–316